

---

# Exact and Approximate Conformal Inference in Multiple Dimensions

---

**Chancellor Johnstone**  
Air Force Institute of Technology

**Eugène Ndiaye**  
Georgia Institute of Technology

## Abstract

It is common in machine learning to estimate a response  $y$  given covariate information  $x$ . However, these predictions alone do not quantify any uncertainty associated with said predictions. One way to overcome this deficiency is with conformal inference methods, which construct a set containing the unobserved response  $y$  with a prescribed probability. Unfortunately, even with one-dimensional responses, conformal inference is computationally expensive despite recent encouraging advances. In this paper, we explore the multidimensional response case within a regression setting, delivering exact derivations of conformal inference  $p$ -values when the predictive model can be described as a linear function of  $y$ . Additionally, we propose different efficient ways of approximating the conformal prediction region for non-linear predictors while preserving computational advantages. We also provide empirical justification for these approaches using a real-world data example.

## 1 Introduction

In regression, we aim to predict (or estimate) some response  $y$  given covariate information  $x$ . These predictions alone deliver no information related to the uncertainty associated with the unobserved response, and thus, would benefit from the inclusion of an interval  $\Gamma^{(\alpha)}(x)$  such that, for  $\alpha \in (0, 1)$ ,

$$\mathbb{P}(y \in \Gamma^{(\alpha)}(x)) = 1 - \alpha. \quad (1)$$

One method to generate  $\Gamma^{(\alpha)}$  is through conformal inference [10, 16], which generates *conservative* prediction intervals for some unobserved response  $y$  under only the assumption of exchangeability of the dataset.

In more complex settings it might be of interest to construct a model for multiple responses, *i.e.*, for some response  $y \in \mathbb{R}^q$ , also known as multi-target (or multi-output) regression [3, 29]. Thus, we might construct a *prediction region* such that some  $q$ -dimension version of  $y$ , say  $y = (y^1, \dots, y^q)'$  is contained within the region.

Unfortunately, even with one-dimensional responses, conformal inference is computationally expensive, with each new candidate point requiring a new model to be fit. Since conformal inference's inception, more efficient methods, *e.g.*, split conformal inference [28, 16], have been introduced with trade-offs between computational efficiency and performance. Other methods, *e.g.*, trimmed conformal inference [7], use a sequential set of models to expedite the search for the conformal prediction region over, say, a grid-based approach.

We contribute the following:

- Extensions of exact conformal inference to multiple dimensions with various predictors and conformity measures.
- The use of numerical root-based methods to find points on the boundary of a multivariate conformal prediction region.
- Methods to provide (convex) approximations of the full conformal prediction region.

The rest of the paper is laid out as follows. Section 2 provides requisite background for the paper. Section 3 extends exact conformal inference to multiple dimensions, while Section 4 introduces the root-based conformal prediction region approximation in multiple dimensions. Section 5 provides empirical evaluation of our proposed approaches. Section 6 concludes the paper.

## 2 Background

In this section we provide background on relevant topics for this paper. Our applications within with paper are focused on regression, so we focus our background discussion on regression as well.

## 2.1 Conformal Inference

Originally introduced in [10] as “transductive inference”, conformal inference (CI) was originally focused on providing inference with classification approaches. [28] provides a formalized introduction to conformal inference within regression. With the express purpose of inference, the goal of CI is to attach, in some fashion, a measure of uncertainty to a predictor, specifically through the construction of a conservative prediction region, *i.e.*, one such that

$$\mathbb{P}(y_{n+1} \in \Gamma^{(\alpha)}(x_{n+1})) \geq 1 - \alpha. \quad (2)$$

We define  $\mathcal{D}_n = \{(x_i, y_i)\}_{i=1}^n$  as a collection of  $n$  observations, where the  $i$ -th data tuple  $(x_i, y_i)$  is made up of a covariate vector  $x_i$  and a response  $y_i$ . We wish to construct a *valid* prediction region for a new observation  $(x_{n+1}, y_{n+1})$ , where  $x_{n+1}$  is some known covariate vector and  $y_{n+1}$  is some, yet-to-be-observed response. Assuming each data pair  $(x_i, y_i)$  and  $(x_{n+1}, y_{n+1})$  are drawn exchangeably from some distribution  $\mathcal{P}$ , conformal inference generates conservative, finite-sample valid prediction regions in a distribution-free manner. Specifically, prediction regions are generated through the repeated inversion of the test,

$$H_0 : y_{n+1} = z \text{ vs. } H_a : y_{n+1} \neq z, \quad (3)$$

where  $z$  is a potential candidate response value, *i.e.*, the null hypothesis [16]. The main approach to perform the test inversion associated with Equation (3) relies on Lemma 1.

**Lemma 1.** *Let  $U_1, \dots, U_n, U_{n+1}$  be an exchangeable sequence of random variables. Then, for any  $\alpha \in (0, 1)$ ,*

$$\mathbb{P}(\text{Rank}(U_{n+1}) \leq \lceil (1 - \alpha)(n + 1) \rceil) \geq 1 - \alpha,$$

where

$$\text{Rank}(U_j) = \sum_{i=1}^{n+1} \mathbb{1}_{U_i \leq U_j}.$$

In a prediction setting, test inversion for a particular candidate value  $z$  is achieved by training the model of interest on an augmented data set  $\mathcal{D}_{n+1}(z) = \mathcal{D}_n \cup (x_{n+1}, z)$ . At this point, we leave our model of interest general, denoting the prediction of the  $i$ -th observation based on a model trained with  $\mathcal{D}_{n+1}(z)$  as  $\hat{y}_i(z)$ .

Following the refitting, each observation in the augmented data set receives a (non)conformity *measure*, which determines the level of (non)conformity between itself and other observations. One popular, and particularly effective, conformity measure is the absolute residual

$$S_i(z) = |y_i - \hat{y}_i(z)|. \quad (4)$$

We can construct the conformity *score* associated with a particular candidate point  $z$  with

$$\pi(z) = \frac{1}{n+1} + \frac{1}{n+1} \sum_{i=1}^n \mathbb{1}\{S_i(z) \leq S_{n+1}(z)\}, \quad (5)$$

where  $S_i(z)$  is the conformity measure for the data pair  $(x_i, y_i)$  as a function of  $z$  and  $S_{n+1}(z)$  is the conformity measure associated with  $(x_{n+1}, z)$ . A prediction region for an unknown response  $y_{n+1}$  associated with some covariate vector  $x_{n+1}$  is

$$\Gamma^{(\alpha)}(x_{n+1}) = \{z : (n+1)\pi(z) \leq \lceil (1 - \alpha)(n+1) \rceil\}. \quad (6)$$

Then, by Lemma 1, with

$$(n+1)\pi(y_{n+1}) \equiv \text{Rank}(S_{n+1}(y_{n+1})),$$

Equation (2) holds for  $\Gamma^{(\alpha)}(x_{n+1})$ . By the previous results, CI can also be utilized in the multivariate response case, where one is interested in quantifying uncertainty with respect to the joint behavior of a collection of responses, given a set of covariates. Thus, we can construct a multi-dimensional prediction region  $\Gamma^{(\alpha)}(x_{n+1}) \subset \mathbb{R}^q$  such that Equation (2) holds when  $y_{n+1}$  is some  $q$ -dimensional random vector.

The first result extending conformal inference to the multivariate setting comes from [15], which applies conformal inference to functional data, providing bounds associated with prediction “bands”. [9] extends and generalizes additional results for conformal inference on functional data. Joint conformal prediction regions outside the functional data setting are explored in [13] and [25]. [19, 20] extend these works through the use of Bonferroni- and copula-based conformal inference, respectively. [6], [12] and [11] construct joint conformal regions through the use of depth measures, *e.g.*, half-space and Mahalanobis depth, as the overall typicalness function.

## 2.2 Efficient conformal inference

Due to the inherent model refitting required to generate prediction regions through full conformal inference, *i.e.*, the testing of an infinite amount candidate points, more computationally efficient methods have been explored, including: conformal inference through resampling [27, 16, 1, 5], exact conformal inference through homotopy [26, 14, 23] and root-finding approaches [24], as well as approximate conformal inference through influence functions [2] and stability-based approaches [22]. We describe a subset of these methods in the following sections. Specifically, we focus on resampling-based and exact conformal inference.

### 2.2.1 Resampling Methods

Split conformal inference [28, 16] generates a conservative prediction intervals under the same assumptions of exchangeability as “full” conformal inference. However, instead of refitting a model for each new candidate value, split conformal inference utilizes a randomly selected partition of  $\mathcal{D}_n$ , which includes a training set  $\mathcal{I}_1$  and a calibration set  $\mathcal{I}_2$ . A prediction model fit using  $\mathcal{I}_1$ . Then, conformity

measures are generated using predictions for observations in  $\mathcal{I}_2$ , where these predictions are generated from the model fitted with  $\mathcal{I}_1$ . The split conformal prediction interval for an incoming  $(x_{n+1}, y_{n+1})$ , when using the absolute residual as our conformity measure, is

$$\Gamma_{\text{split}}^{(\alpha)}(x_{n+1}) = [\hat{y}_{n+1} - s, \hat{y}_{n+1} + s], \quad (7)$$

where  $\hat{y}_{n+1}$  is the prediction for  $y_{n+1}$  generated using the observations in  $\mathcal{I}_1$ , and  $s$  is the  $\lceil (|\mathcal{I}_2| + 1)(1 - \alpha) \rceil$ -th largest conformity measure for observations in  $\mathcal{I}_2$ .

In order to combat the larger widths and high variance associated with split conformal intervals, cross-validation (CV) approaches to conformal inference have also been implemented. The first CV approach was introduced in [27] as cross-conformal inference with the goal to “smooth” inductive conformity scores across multiple folds. Aggregated conformal predictors [5] generalize cross-conformal predictors, constructing prediction intervals through any exchangeable resampling method, *e.g.*, bootstrap resampling.

For a more detailed review and empirical comparison of resampling-based conformal inference methods, we point the interested reader to [8].

### 2.2.2 Exact Conformal Inference

In order to test a particular candidate values for inclusion in  $\Gamma^{(\alpha)}(x_{n+1})$ , we need to compare the conformity measure associated with our candidate data point to the conformity measures of our training data. Naively, this requires the re-fitting of our model for each new candidate value. However, [26] showed that  $S_i(z)$ , constructed using Equation (4) in conjunction with a ridge regressor, varied piecewise-linearly as a function of the candidate value  $z$ , eliminating the need to test a fine set of candidate points through model refitting. We provide this result in Lemma 2.

**Lemma 2.** *Assume the fitted model  $\hat{y}_i = x_i' \hat{\beta}$ ,*

*where  $\hat{\beta} = \arg \min_{\beta} \|y - X\beta\|_2^2 + \lambda \|\beta\|_2^2$ . Then,*

$$S_i(z) = |a_i + b_i z|,$$

*where  $a_i$  and  $b_i$  are the  $i$ -th elements of the vectors  $A$  and  $B$ , respectively, with*

$$\begin{aligned} A &= (I - X(X'X + \lambda I)^{-1}X')(y, 0)', \\ B &= (I - X(X'X + \lambda I)^{-1}X')(0, \dots, 0, 1), \end{aligned}$$

*where  $X$  includes  $x_{n+1}$ .*

Lemma 2 was extended to include both lasso and elastic net regressors in [14]. For this paper, we focus on ridge regression and other similar approaches using a generalized version of Lemma 2, shown in Lemma 3.

**Lemma 3.** *Assume the fitted model  $\hat{y}_i = (H(x_{n+1}, x_i)y)_i'$ , where  $H(x_{n+1}, x)$  is an  $(n+1) \times (n+1)$  matrix generated*

*as a function of  $x_{n+1}$  and some  $x_i$ . Then, with Equation (4) as our conformity measure,*

$$S_i(z) = |a_i + b_i z|,$$

*where  $a_i$  and  $b_i$  are the  $i$ -th elements of the vectors  $A$  and  $B$ , respectively, with*

$$\begin{aligned} A &= (I - H(x_{n+1}, x_i))(y, 0)' \\ B &= (I - H(x_{n+1}, x_i))(0, \dots, 0, 1). \end{aligned}$$

We omit the proof of Lemma 3 as it follows closely the proof shown in [26]. While Lemma 3 allows for  $H(x_{n+1}, x_i)$  to be dependent explicitly on  $x_{n+1}$  and  $x_i$ , we omit dependence on  $x_i$  for notational ease. We discuss predictors with specific dependence on  $x_i$  in Section 5.

## 3 Exact Conformal $p$ -values in Multiple Dimensions

In the following sections, we extend the results in Section 2.2.2 to multiple dimensions. We also discuss closed-form solutions for higher dimension prediction regions with other conformity measures.

While CI can be applied to any prediction or classification task, we restrict each of our predictors to the form

$$\hat{y}_{ik}(z) = (H_k(x_{n+1})y_k(z))_i, \quad (8)$$

where  $y_{ik}(z)$  is the  $i$ -th element of  $y_k(z) = (y_{1k}, \dots, y_{nk}, z)'$ . Additionally, we require that  $H_k$  be independent of  $y_k$ . Even with this restriction,  $H_k$  is general enough so as to include many classes of predictors. For the case of ridge regression,  $H_k$  is of the form,

$$H_k(x_{n+1}) = X(X'X + \lambda_k I)^{-1}X', \quad (9)$$

where  $X$  includes  $x_{n+1}$ .

### 3.1 Exact $p$ -values with $\|\cdot\|_1$

Without loss of generality, we first consider the two-dimensional case with a conformity measure similar to that utilized in [26]. More specifically, we utilize

$$S_i(z) = \|y_i - \hat{y}_i(z)\|_1, \quad (10)$$

as our conformity measure, with our candidate point  $z = (z_1, z_2)'$ , our response vector  $y_i = (y_{i1}, y_{i2})'$  and the vector of predictions  $\hat{y}_i(z) = (\hat{y}_{i1}(z_1), \hat{y}_{i2}(z_2))'$ . We can extend the closed-form solution of [26] to multiple dimensions by applying Lemma 3 to each dimension, resulting in the conformity measure

$$S_i(z) = |a_{1i} - b_{1i}z_1| + |a_{2i} - b_{2i}z_2|, \quad (11)$$

where  $a_{ki}$  and  $b_{ki}$  are the  $i$ -th elements of the vectors  $A_k$  and  $B_k$ , respectively, with

$$A_k = (I - H_k(x_{n+1}))(y_k, 0)', \quad (12)$$

and,

$$B_k = (I - H_k(x_{n+1}))(0, \dots, 0, 1). \quad (13)$$

Then, changes in the  $p$ -value associated with a candidate point are only observed when  $S_i(z) = S_{n+1}(z)$ .

In the one-dimensional case, we only need to consider at most two points of intersection between  $S_i$  and  $S_{n+1}$ ,

$$z = \frac{a_i - a_{n+1}}{b_{n+1} - b_i} \text{ and } z = -\frac{a_i + a_{n+1}}{b_i + b_{n+1}}. \quad (14)$$

In contrast, the two-dimensional case requires the consideration of  $2^4$  different equations; for each additional dimension  $k$  we include  $|a_{ki} + b_{ki}y_k|$  and  $|a_{kn+1} + b_{kn+1}y_k|$  terms within our conformity measures for observations  $i$  and  $n+1$ , respectively. As an example, we can construct one possible  $p$ -value change point set by first considering solutions to

$$(a_{1i} + b_{1i}z_1) + (a_{2i} + b_{2i}z_2) = (a_{1n+1} + b_{1n+1}z_1) + (a_{2n+1} + b_{2n+1}z_2), \quad (15)$$

which yields the solution

$$z_1 = \frac{(a_{1n+1} - a_{1i}) + (a_{2n+1} - a_{2i}) + (b_{2n+1} - b_{2i})z_2}{b_{1i} - b_{1n+1}}.$$

We can describe all of the potential intersection sets by adjusting each term in Equation (15) to take on either its positive or negative version. The  $2^4$  possible combinations associated with Equation (15) are shown in Supplementary Materials. The possible intersection sets for a real-world data example using linear regression are shown in Figure 1.

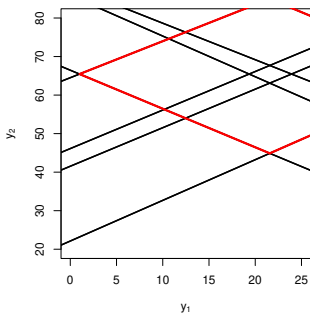
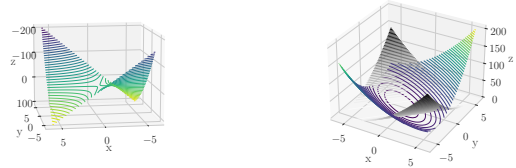


Figure 1: Real data example showing possible intersections of  $S_i$  and  $S_{n+1}$  (black) and true intersections of  $S_i$  and  $S_{n+1}$  (red). Constructed using linear regression.

We formalize the two dimensional result in Equation (11) to  $d$  dimensions in Proposition 1.



(a) Plot of the difference  $\psi_1 - \psi_2$       (b) Plot of  $\psi_1$  and  $\psi_2$

Figure 2:  $\psi_1 : h \mapsto \|y_0 - T_1 h\|$  and  $\psi_2 : h \mapsto \|T_2 h\|$  where  $y_0 = (1, 0)'$ ,  $T_1 = \begin{pmatrix} -1 & -1 \\ -1 & 0 \end{pmatrix}$  and  $T_2 = \begin{pmatrix} 0 & -1 \\ 0 & 1 \end{pmatrix}$ .

**Proposition 1.** Assume the fitted model,  $\hat{y}_i(z) = (H(x_{n+1})y(z))_i$ , then, using Equation (10),

$$S_i(z) = \|a_i + b_i z\|_1,$$

where  $a_i = (a_{1i}, \dots, a_{di})'$ ,  $b_i = (b_{1i}, \dots, b_{di})'$ , and  $a_{ki}$  and  $b_{ki}$  are the  $i$ -th elements of the vectors  $A_k$  and  $B_k$ , respectively, as defined in Equation (12) and Equation (13).

Using Proposition 1 for each observation  $(x_i, y_i)$ , we can generate a collection of regions,  $\mathcal{E} = \{\mathcal{E}_i\}_{i=1}^n$ , where

$$\mathcal{E}_i \equiv \{z \in \mathbb{R}^d : S_{n+1}(z) \leq S_i(z)\}.$$

For completeness, we can explicitly define  $\mathcal{E}_{n+1} \equiv \mathbb{R}^d$ . We provide the detailed Algorithm in Supplemental Materials to construct these regions. Then, the  $p$ -value associated with the hypothesis test shown in Equation (3) for any candidate point  $z$  is

$$p\text{-value}(z) = \frac{|\{i \in 1, \dots, n : z \in \mathcal{E}_i\}|}{n + 1}. \quad (16)$$

With Equation (16), we can generate exact  $p$ -values for any candidate value  $z$  by only training our predictor(s) once. It is important to note that the  $p$ -value change points we construct in one dimension with Lemma 3 directly translate to the exact conformal prediction regions. This is not the case in multiple dimensions.

### 3.2 Exact $p$ -values with $\|\cdot\|_W^2$

In order to generalize our exact  $p$ -value construction further than for use solely with  $\|\cdot\|_1$ , we now consider conformity measures of the form

$$S_i(z) = r_i(z)' W r_i(z) \equiv \|r_i(z)\|_W^2, \quad (17)$$

where  $r_i(z) = y_i - \hat{y}_i(z)$ ,  $y_i = (y_{i1}, \dots, y_{id})'$  and  $W$  is some  $d \times d$  matrix. In one dimension, if we select  $W \equiv I$ , Equation (17) reduces to

$$S_i(z) = r_{n+1}^2(z), \quad (18)$$

which results in the same conformal prediction regions as using Equation (4) for our conformity measure. Proposition

2 provides a similar result to Lemma 3 when using Equation (17) in one dimension. Namely,  $S_i$  becomes quadratic with respect to  $z$ , instead of piecewise-linear. In one dimension, the conformity measure for the  $i$ -th observation is

$$S_i(z) = (a_i + b_i z)^2,$$

where  $a_i$  and  $b_i$  are the  $i$ -th elements of the vectors  $A$  and  $B$ , respectively, as defined in Lemma 3.

Due to the quadratic nature of the conformity measures for each observation, we can analytically solve for all candidate points where the conformity measure for  $z$  is smaller than the conformity measure for observation  $i$ . Proposition 2 extends these results to  $d$ -dimensions.

**Proposition 2.** *Assume the fitted model*

$$\hat{y}_{ik}(z) = (H_k(x_{n+1})y_k(z))_i,$$

for each response dimension  $k \in 1, \dots, d$ . Then, using Equation (17),

$$S_i(z) = \begin{bmatrix} a_{1i} + b_{1i}z_1 \\ \vdots \\ a_{di} + b_{di}z_d \end{bmatrix}' W \begin{bmatrix} a_{1i} + b_{1i}z_1 \\ \vdots \\ a_{di} + b_{di}z_d \end{bmatrix}$$

where  $W$  is some  $d \times d$  matrix and  $a_{ki}$  and  $b_{ki}$  are the  $i$ -th elements of the vectors  $A_k$  and  $B_k$ , respectively, as defined in Equation (12) and Equation (13).

In order to maintain the probabilistic guarantees inherent to conformal inference, we require  $W$  to be constructed exchangeably. Two constructions that satisfy exchangeability are: 1)  $W$  independent of  $\mathcal{D}_{n+1}$ , or 2)  $W$  must utilize all observations within  $\mathcal{D}_{n+1}(z)$ . However, we show in Section 5 that, in practice, setting  $W \equiv \hat{\Sigma}^{-1}$ , the observed inverse covariance matrix associated with the residuals from our  $d$  responses from a model constructed using only  $\mathcal{D}_n$ , performs well.

While Proposition 2 does not restrict the structure of  $W$ , limiting  $W$  to be positive semi-definite ensures that the set  $\mathcal{E}_i$ , defined in the same fashion as in Section 3.1, is not only convex, but ellipsoidal. Without this additional restriction on the matrix  $W$ , these intersection sets could be ill-formed, i.e., nonconvex. An example of an ill-formed intersection set is shown in Figure 2. The  $p$ -value associated with some  $z$  using sets constructed using Equation (17) is the same as in Equation (16).

### 3.3 Approximation of Conformal Prediction Regions

While the results in Section 3.1 and Section 3.2 allow for the construction of exact  $p$ -values with no additional model refitting (for multiple responses), we still cannot describe exact conformal prediction regions in closed-form. It is initially unclear which regions  $\mathcal{E}_k$  make up various conformal

prediction sets, let alone how we need to combine these regions to get the exact conformal prediction sets.

Thus, we aim to provide an approximation of conformal prediction sets using the regions generated with either of the approaches in Section 3.1 or Section 3.2. We provide Proposition 3 to bound error probabilities associated with potential combinations of these regions.

**Proposition 3.** *Under uniqueness of conformity measures, for some  $y \in \mathbb{R}^d$  such that  $(x_1, y_1), \dots, (x_{n+1}, y)$  are drawn exchangeably from  $\mathcal{P}$ ,*

$$\mathbb{P}\left(y \in \bigcup_{i \in \mathcal{S}} \mathcal{E}_i\right) \geq \frac{|\mathcal{S}|}{n+1}$$

for any  $\mathcal{S} \subset \{1, \dots, n\}$ .

Proposition 3 states that with the selection of *any* subset of  $\mathcal{E}$ , the probability of a response  $y$  being contained in that subset is bounded-below by a function of cardinality. For example, if we wish to construct, say, a conservative 50% prediction region, we could select any subset  $\mathcal{S} \subseteq \mathcal{E}$  such that  $|\mathcal{S}| \geq |\mathcal{E}|/2$ . Now, this may not be a particularly tight bound as there might exist some  $\mathcal{E}_i$  such that

$$\bigcup_{i' \in \mathcal{S}_{(i)}} \mathcal{E}_{i'} \subseteq \mathcal{E}_i,$$

where  $\mathcal{S}_{(i)}$  is any subset of  $\mathcal{I}$  that does not contain  $i$ , meaning some sets are contained in others and, thus, choosing *only* the containing set could result in probabilities much larger than the lower bound identified in Proposition 3.

To reduce the conservativeness of our constructed region, we can provide more intelligently constructed regions that are empirically less conservative (but still valid) than, say, the union of a random selection of regions to form a  $1 - |\mathcal{S}|/(n+1)$  prediction region. Suppose we provide an ordering of our regions, where  $\mathcal{E}_{(k)}$  is defined as the  $k$ -th smallest region by volume. Then, a more efficient  $(1 - \alpha)$  prediction region approximation can then be constructed as

$$\hat{\Gamma}^{(\alpha)}(x_{n+1}) = \bigcup_{i \in \mathcal{S}_\alpha} \mathcal{E}_{(i)}, \quad (19)$$

where  $\mathcal{S}_\alpha = \{1, \dots, \lceil (1 - \alpha)(n+1) \rceil\}$ .

We compare prediction regions constructed using Equation (19), as well as a random selection of regions for multiple predictors in Section 5. We also include results related to the theoretical coverage probabilities associated with the randomized approach in Supplemental Materials.

While Proposition 3 and the adjustment described in Equation (19) allows for conservative prediction regions, at times, the union of various  $\mathcal{E}_i$  does not explicitly describe a conformal prediction region exactly. Thus, this approach is (at worse) a conservative approximation of the true conformal

prediction region. Because we have reduced the computations required to generate exact  $p$ -values, a grid-based approach to determine  $p$ -values for a fine collection of candidate points could be used with much computational gain over that of full conformal prediction.

## 4 Root-based Approximation Methods

As seen earlier, the computation of the conformal prediction sets requires to readjust a predictive model for any candidate to replace the true  $y_{n+1}$  value. Current efficient approaches to exact computation, limited to dimension one, are restricted to models that are piecewise linear. This structure allows to track changes in the conformity function. We have extended these approaches to higher dimensions in the previous section.

To go beyond linear structures, we can use approximate homotopy approaches which, given an optimization tolerance, provide a discretization of all the values that  $y_{n+1}$  can take. However, these approaches are also limited in dimension one and have an exponential complexity in the dimension of  $y_{n+1}$ . Convexity assumptions are also required, which, unfortunately, are not verified for more complex prediction models.

In this section, we extend the approximations of conformal prediction in multiple dimensions by computing boundaries directly. Unlike the one-dimensional case where the boundary is simply two points, in multiple dimensions the boundary is often continuous and so uncountable, which makes finite-time computations quite impossible. To get around this difficulty, the main idea here is very simple. We will first fix a finite set of search directions on which we will estimate the intersection points between the boundary of the conformal prediction set and the chosen direction. Then, we use the points on the boundary as a data base to fit a convex set, *e.g.*, an ellipse or the convex hull, passing through these points. More formally, we want to estimate (efficiently) the set described in Equation (6).

**Assumptions.** We suppose that the conformal prediction set is star shaped *i.e.*, it exists a point  $z_0$  such that any other conformal point  $z$  can be connected to  $z_0$  with a line segment entirely drawn in  $\Gamma^{(\alpha)}(x_{n+1})$ .

Note that a star shaped set can be non-convex so that we can still approximate complex conformal sets. We provide some illustration in Figure 4.

### Outline of the Root-Based Algorithm

Given any direction  $d \in \mathbb{R}^q$ , the intersection points between  $\partial\Gamma^{(\alpha)}(x_{n+1})$ , defined as the boundary of  $\Gamma^{(\alpha)}(x_{n+1})$ , and the line passing through  $z_0$  and directed by  $d$  are obtained

by solving the one dimensional equation

$$\pi(z(t, d)) = 1 - \alpha, \quad (20)$$

where the test points  $z(t, d) = z_0 + td, t \in \mathbb{R}$  are restricted on a line. We briefly described the main steps and display the detailed algorithm in the appendix.

1. Fit a model  $\mu_0$  on the observed training set  $\mathcal{D}_n$  and predict a feasible point  $z_0 = \mu_0(x_{n+1})$ .
2. For a collection of search directions  $\{d_1, \dots, d_K\}$ , perform a bisection search in  $[t_{\min}, 0]$  and  $[0, t_{\max}]$  to output solutions  $\hat{\ell}(d_k)$  and  $\hat{u}(d_k)$  of Equation (20) at direction  $d_k$ , after at most  $\log_2(\frac{t_{\max} - t_{\min}}{\epsilon_r})$  iterations for an optimization tolerance  $\epsilon_r > 0$ . Notice that the star-shape hypothesis implies that we will have only two roots on the selected directions.
3. Fit a convex set on the roots obtained at the previous step  $\{\hat{\ell}(d_k), \hat{u}(d_k)\}_{k \in [K]}$ . In practice, when one uses a least-squares ellipse as the convex approximate, a number of search directions  $K$  is proportional to the dimension  $q$  of the target  $y_{n+1}$ , is sufficient. This is not necessarily the case for the convex hull. We refer to Figure 4 where we observe that many more search directions are needed to cover the conformal set.

## 5 Empirical Results and Application

To provide empirical support for our theoretical results, we consider a small data example using the multi-target concrete data set [30]. For the sake of simplicity, we limit our exploration to two dimensions, focusing on the construction of prediction regions for slump and flow, given information on other elements in the mixture, *e.g.*, amount of cement, fly ash and superplasticizer.

We include empirical coverage results for the approximation approaches described in Section 3, specifically with regions constructed using  $\|\cdot\|_W^2$ . We also include results for the root-based approximation results described in Section 4 for a wide-array of predictors that include those more general than the restrictions we outline in our paper.

### $H(x_{n+1})$ through Kernel Regression with Application

We can construct various  $H(x_{n+1})$  matrices that allow for exact  $p$ -values using kernel regression. First, consider the Nadaraya-Watson estimator [21] which, for some  $x_i$  in  $\mathcal{D}_{n+1}(z)$ , generates a prediction

$$\hat{y}_i = \sum_{j=1}^{n+1} \frac{K_h(x_j - x_i)}{\sum_{j=1}^{n+1} K_h(x_j - x_i)} y(z),$$

where  $K_h(x_i)$  is the (product) kernel estimate associated with  $x_i$  and bandwidth vector  $h$  resulting in a

$$H(x_{n+1}) = (w_1, \dots, w_{n+1})',$$

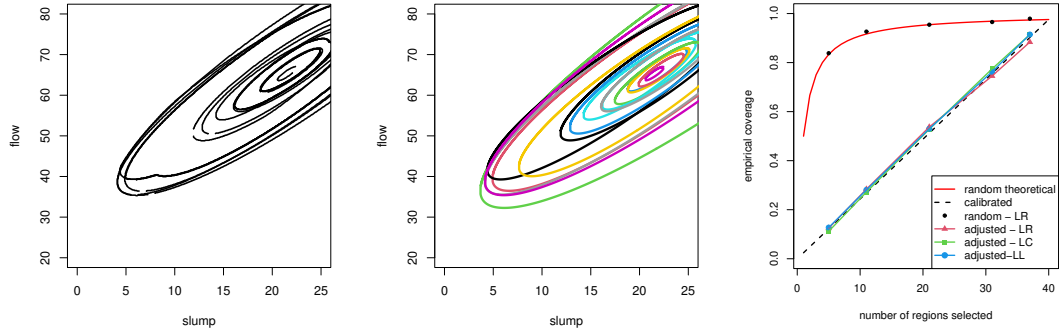


Figure 3: Comparing grid-based conformal prediction regions (left) to closed-form  $p$ -value change point regions (middle) constructed using  $\|\cdot\|_W^2$ . Comparison of empirical coverage with random selection of  $k$  regions and adjusted variant described in Equation (19) for various predictors, including: linear regression (LR), Nadaraya-Watson (LC), and local-linear (LL) across 100 repetitions (right). The calibrated curve is constructed using  $number\ of\ regions / (n + 1)$ .

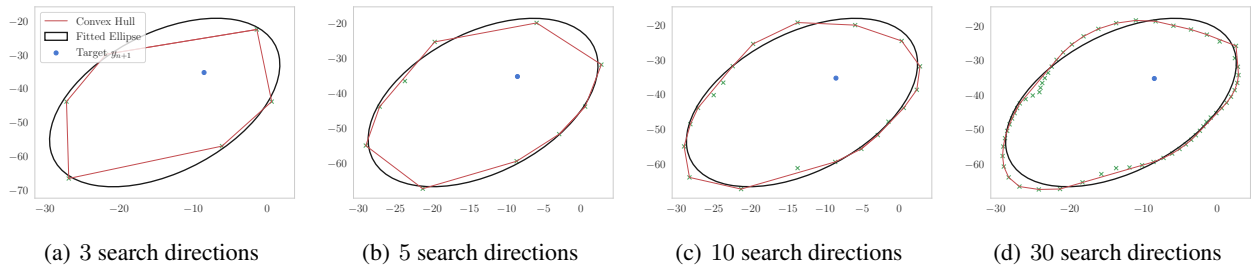


Figure 4: Illustration of the conformal set obtained fitting ellipse and convex hull given boundary points obtained by root-finding methods. We use scikit-learn `make_regression` to generate synthetic dataset with the parameters `n_samples = 15`, `n_features = 5`, `n_targets = 2` is the dimension of in output  $y_{n+1}$ . We selected 80% of informative features and 60% for effective rank (described as the approximate number of singular vectors required to explain most of the input data by linear combinations) and the standard deviation of the random noise is set to 5.

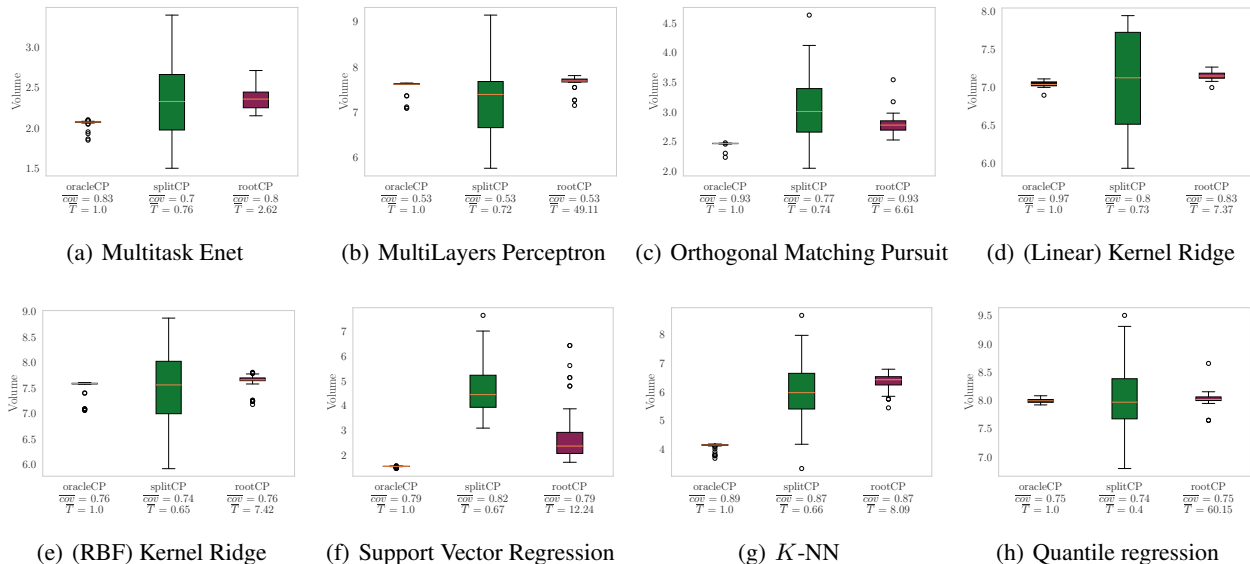


Figure 5: Ellipse Benchmarking conformal sets for several regression models on cement dataset. We display the lengths of the confidence sets over 100 random permutation of the data. We denoted  $\overline{cov}$  the average coverage, and  $\overline{T}$  the average computational time normalized with the average time for computing `oracleCP` which requires a single model fit on the whole data.

with  $w_i$  defined as the normalized vector of individual kernel elements centered on  $x_i$ . We also consider an  $H(x_{n+1}, x_i)$  constructed through local-linear regression, with

$$H(x_{n+1}, x_i) = \tilde{X}_i (\tilde{X}_i' G(x_i) \tilde{X}_i)^{-1} \tilde{X}_i' G(x_i),$$

where  $G(x_i)$  is the diagonal kernel matrix centered on  $x_i$  and  $\tilde{X}_i$  is

$$\tilde{X}_i = \begin{bmatrix} 1 & (x_1 - x_i)' \\ \vdots & \vdots \\ 1 & (x_{n+1} - x_i)' \end{bmatrix}.$$

Both the Nadaraya-Watson and local linear estimators follow the predictor restrictions laid out in Section 2.2.2, allowing us to 1) construct exact  $p$ -values and 2) approximate the conformal prediction regions using the methods laid out in Section 3.3.

Figure 3 includes a comparison of the  $p$ -value change point regions constructed with (17) to the conformal prediction regions constructed using the grid-based approach, also with linear regression for each predictor as well as coverage results for various predictors on the concrete data set. From Figure 3, we can see that our approximations are empirically calibrated.

### Root-Based Approximation Application

We numerically examine the performance of the root-finding methods to compute various conformal prediction sets for regression problems on both synthetic, and real

databases. The experiments were conducted with a coverage level of 0.9, *i.e.*,  $\alpha = 0.1$ . For comparisons, we run the evaluations on 100 repetitions of examples, and display the average of the following performance statistics for different methods: 1) the empirical coverage, *i.e.*, the percentage of times the prediction set contains the held-out target  $y_{n+1}$ , 2) the volume of the confidence intervals, and 3) the execution time. For each run, we randomly select a data tuple  $(x_i, y_i)$  to constitute the targeted variables for which we will compute the conformal prediction set. The rest is considered as observed data  $\mathcal{D}_n$ . Similar experimental setting was considered in [14].

As a reference benchmark, from Lemma 1, we have  $\pi(y_{n+1}) \geq \alpha$  with probability larger than  $1 - \alpha$ . Whence one can define the `OracleCP` as  $\pi^{-1}([\alpha, +\infty))$  where  $\pi$  is obtained with a model fit optimized on the oracle data  $\mathcal{D}_{n+1}(y_{n+1})$  on top of the root-based approach to find boundary points. We remind the reader that the target variable  $y_{n+1}$  is not available in practice.

We run experiments on more complex regression models, including: MultiTask Elastic Net, Multi-Layers Perceptron, Orthogonal Matching Pursuit, Kernel Ridge regression with both linear and Gaussian kernel, Support Vector Regression,  $K$ -nearest neighbor and Quantile regression. The results are shown in Figure S5.



## 6 Conclusion

In this paper, we introduced exact  $p$ -values in multiple dimensions for predictors that are a linear function of the candidate value. Specifically, we discussed the exact construction of  $p$ -values using various conformity measures to include  $\|\cdot\|_1$  and  $\|\cdot\|_W^2$ . Additionally, we introduced methods for generating convex and non-convex approximations of multidimensional  $1 - \alpha$  conformal prediction regions through root-based and union-based prediction region construction, respectively, also delivering probabilistic bounds and convergence results for these approximations. We then showed empirically with multiple predictors, including a subset of both linear and nonlinear predictors, that these approximations were comparable to the grid-based full conformal prediction regions, while drastically reducing the computational requirements.

Future work could involve further exploration of various constructions of  $H(x_{n+1}, x_i)$ . As an example, it is well known that random forests [4] provide predictions which can be described as

$$\hat{y}_i = w(x_i)'y,$$

where  $w(x_i)$  is constructed based on the appearance of training data covariates  $x_1, \dots, x_n$  with the point of interest  $x_i$  in terminal nodes [17, 18]. Adjustment of the random forest procedure to generate  $w(x_i)$  exchangeably with some  $(x_{n+1}, z)$  would reduce the computation required to generate  $p$ -values and potentially reduce variability due to randomization inherent to the procedure.

We also hope to further explore other approximation approaches and how they can be used in decision-making under uncertainty, e.g., a robust optimization setting.

## References

- [1] Rina Foygel Barber et al. “Predictive inference with the jackknife+”. In: *The Annals of Statistics* 49.1 (2021), pp. 486–507.
- [2] Umang Bhatt, Adrian Weller, and Giovanni Cherubin. “Fast conformal classification using influence functions”. In: *Conformal and Probabilistic Prediction and Applications*. PMLR. 2021, pp. 303–305.
- [3] Hanen Borchani et al. “A survey on multi-output regression”. In: *Wiley Interdisciplinary Reviews: Data Mining and Knowledge Discovery* 5.5 (2015), pp. 216–233.
- [4] Leo Breiman. “Random forests”. In: *Machine learning* 45.1 (2001), pp. 5–32.
- [5] Lars Carlsson, Martin Eklund, and Ulf Norinder. “Aggregated conformal prediction”. In: *IFIP International Conference on Artificial Intelligence Applications and Innovations*. Springer. 2014, pp. 231–240.
- [6] Leonardo Cella and Ryan Martin. “Valid distribution-free inferential models for prediction”. In: *arXiv preprint arXiv:2001.09225* (2020).
- [7] Wenyu Chen et al. “Trimmed conformal prediction for high-dimensional models”. In: *arXiv preprint arXiv:1611.09933* (2016).
- [8] Alex Contarino et al. “Constructing prediction intervals with neural networks: an empirical evaluation of bootstrapping and conformal inference methods”. In: *arXiv preprint arXiv:2210.05354* (2022).
- [9] Jacopo Diquigiovanni, Matteo Fontana, and Simone Vantini. “Conformal Prediction Bands for Multivariate Functional Data”. In: *arXiv preprint arXiv:2106.01792* (2021).
- [10] Alexander Gammerman, Vladimir Vovk, and Vladimir Vapnik. “Learning by transduction”. In: *Proceedings of the Fourteenth conference on Uncertainty in artificial intelligence*. 1998, pp. 148–155.
- [11] Chancellor Johnstone and Bruce Cox. “Conformal uncertainty sets for robust optimization”. In: *Conformal and Probabilistic Prediction and Applications*. PMLR. 2021, pp. 72–90.
- [12] Arun Kumar Kuchibhotla. “Exchangeability, Conformal Prediction, and Rank Tests”. In: *arXiv preprint arXiv:2005.06095* (2020).
- [13] Alexander Kuleshov, Alexander Bernstein, and Evgeny Burnaev. “Conformal prediction in manifold learning”. In: *Conformal and Probabilistic Prediction and Applications*. 2018, pp. 234–253.
- [14] Jing Lei. “Fast exact conformalization of the lasso using piecewise linear homotopy”. In: *Biometrika* 106.4 (2019), pp. 749–764.
- [15] Jing Lei, Alessandro Rinaldo, and Larry Wasserman. “A conformal prediction approach to explore functional data”. In: *Annals of Mathematics and Artificial Intelligence* 74.1 (2015), pp. 29–43.
- [16] Jing Lei et al. “Distribution-free predictive inference for regression”. In: *Journal of the American Statistical Association* 113.523 (2018), pp. 1094–1111.
- [17] Yi Lin and Yongho Jeon. “Random forests and adaptive nearest neighbors”. In: *Journal of the American Statistical Association* 101.474 (2006), pp. 578–590.
- [18] Nicolai Meinshausen and Greg Ridgeway. “Quantile regression forests.” In: *Journal of machine learning research* 7.6 (2006).
- [19] Soundouss Messoudi, Sébastien Destercke, and Sylvain Rousseau. “Conformal multi-target regression using neural networks”. In: *Conformal and Probabilistic Prediction and Applications*. PMLR. 2020, pp. 65–83.
- [20] Soundouss Messoudi, Sébastien Destercke, and Sylvain Rousseau. “Copula-based conformal prediction for Multi-Target Regression”. In: *arXiv preprint arXiv:2101.12002* (2021).

- [21] EA Nadaraya. “On non-parametric estimates of density functions and regression curves”. In: *Theory of Probability & Its Applications* 10.1 (1965), pp. 186–190.
- [22] Eugene Ndiaye. “Stable Conformal Prediction Sets”. In: *International Conference on Machine Learning*. PMLR, 2022, pp. 16462–16479.
- [23] Eugene Ndiaye and Ichiro Takeuchi. “Computing full conformal prediction set with approximate homotopy”. In: *arXiv preprint arXiv:1909.09365* (2019).
- [24] Eugene Ndiaye and Ichiro Takeuchi. “Root-finding Approaches for Computing Conformal Prediction Set”. In: *arXiv preprint arXiv:2104.06648* (2021).
- [25] Jelmer Neeven and Evgueni Smirnov. “Conformal stacked weather forecasting”. In: *Conformal and Probabilistic Prediction and Applications*. 2018, pp. 220–233.
- [26] Ilia Nouretdinov, Thomas Melliush, and Volodya Vovk. “Ridge regression confidence machine”. In: *ICML*. Citeseer, 2001, pp. 385–392.
- [27] Vladimir Vovk. “Cross-conformal predictors”. In: *Annals of Mathematics and Artificial Intelligence* 74.1 (2015), pp. 9–28.
- [28] Vladimir Vovk, Alex Gammerman, and Glenn Shafer. *Algorithmic learning in a random world*. Springer Science & Business Media, 2005.
- [29] Donna Xu et al. “Survey on multi-output learning”. In: *IEEE transactions on neural networks and learning systems* 31.7 (2019), pp. 2409–2429.
- [30] I-Cheng Yeh. “Modeling slump flow of concrete using second-order regressions and artificial neural networks”. In: *Cement and concrete composites* 29.6 (2007), pp. 474–480.

## Supplemental Materials

In the following sections, we provide proofs of the main proposals of the paper, and we provide some additional numerical experiments to illustrate the performance of the proposed algorithms. We also propose detailed pseudo code of the latter.

### S.1 Proofs

#### S.1.1 Proof of Proposition 2

*Proof.* The proof follows directly from applying Lemma 3 to each element of the vector. □

#### S.1.2 Proof of Proposition 3

*Proof.* Assume we have the data pair  $(x, y)$  drawn exchangeably with  $(x_1, y_1), \dots, (x_n, y_n)$ . Also assume that we have constructed  $\mathcal{E}$ . First, we select and fix any  $\mathcal{S} \subseteq \mathcal{I}$ . We then fix a  $z$  such that  $z \notin \bigcup_{i \in \mathcal{S}} \mathcal{E}_i$ . Then,

$$\begin{aligned} z \notin \bigcup_{i \in \mathcal{S}} \mathcal{E}_i &\implies S_i(z) \leq S_{n+1}(z) \quad \forall i \in \mathcal{S} \\ &\implies \mathbb{1}\{S_i(z) \leq S_{n+1}(z)\} = 1 \quad \forall i \in \mathcal{S} \\ &\implies \sum_{i=1}^{n+1} \mathbb{1}\{S_i(z) \leq S_{n+1}(z)\} \geq |\mathcal{S}| + 1 \end{aligned}$$

Then, for  $y$

$$\begin{aligned} \mathbb{P}\left(y \notin \bigcup_{i \in \mathcal{S}} \mathcal{E}_i\right) &= \mathbb{P}\left(\sum_{i=1}^{n+1} \mathbb{1}\{S_i(y) \leq S_{n+1}(y)\} \geq |\mathcal{S}| + 1\right) \\ \implies \mathbb{P}\left(y \in \bigcup_{i \in \mathcal{S}} \mathcal{E}_i\right) &= 1 - \mathbb{P}\left(\sum_{i=1}^{n+1} \mathbb{1}\{S_i(y) \leq S_{n+1}(y)\} \geq |\mathcal{S}| + 1\right) \\ &= \mathbb{P}\left(\sum_{i=1}^{n+1} \mathbb{1}\{S_i(y) \leq S_{n+1}(y)\} \leq |\mathcal{S}|\right). \end{aligned}$$

By Lemma 1, with the selection of  $\alpha = 1 - \frac{|\mathcal{S}|}{n+1}$ ,

$$\mathbb{P}\left(\sum_{i=1}^{n+1} \mathbb{1}\{S_i(y) \leq S_{n+1}(y)\} \leq |\mathcal{S}|\right) \geq \frac{|\mathcal{S}|}{n+1},$$

which completes the proof. □

#### S.1.3 Sketch-Proof of Random Region Selection Coverage Probability

We now include a sketch-proof for the probability that a randomly selected subset of  $\mathcal{E}_{i=1}^n$ , of size  $k$ , constructed with  $\mathcal{D}_{n+1}(z)$  will contain  $y_{n+1}$ .

*Proof.* First, we define  $\Gamma_k$  as a random subset of size  $k$  where each region  $i$ , constructed as a function of  $\mathcal{D}_{n+1}(z)$ , is selected with probability  $1/n$ . We assume, without loss of generality that  $\mathcal{E}_{(i)} \subset \mathcal{E}_{(i+1)} \forall i = 1, \dots, n$ . While this assumption does not always hold, it results in a larger upper bound. Then, for  $y_{n+1}$ ,

$$\mathbb{P}(y_{n+1} \in \mathcal{E}_{(k)}) = \frac{k}{n+1} \tag{21}$$

Furthermore, let the random variable  $e_i = 1$  if region  $\mathcal{E}_{(i)}$  is selected (with probability  $1/n$ ). Then, for  $k = 1$ ,

$$\begin{aligned}
 \mathbb{P}(y_{n+1} \in \Gamma_1) &= \sum_{i=1}^n \mathbb{P}(y_{n+1} \in \Gamma_1, e_i = 1) \\
 &= \sum_{i=1}^n \mathbb{P}(y_{n+1} \in \Gamma_1 | e_i = 1) \mathbb{P}(e_i = 1) \\
 &= \frac{1}{n} \sum_{i=1}^n \mathbb{P}(y_{n+1} \in \Gamma_1 | e_i = 1) \\
 &= \frac{1}{n} \sum_{i=1}^n \frac{i}{n+1} && \text{(by (21))} \\
 &= \frac{1}{n(n+1)} \sum_{i=1}^n i \\
 &= \frac{1}{n(n+1)} \frac{n(n+1)}{2} \\
 &= \frac{1}{2}
 \end{aligned}$$

Now consider  $\Gamma_k$  for  $k > 1$ . We define the random variable  $\pi_k$  as a joint random variable for  $(e_1, \dots, e_n)$  where the support of  $\pi_k$  is  $\Pi_k$ , the set of all  $2^n$  combinations of  $e_i \in \{0, 1\}$ . Because we limit our regions to be nested, the  $(k)$ -th region is contained in  $(k+1)$ -th region. Thus, we can succinctly describe probabilities associated with various  $\Gamma_k$  and  $\pi_k$  by just examining the highest  $k$  such that  $e_k = 1$ , defined as  $\max_k(\pi_k)$ . Then,

$$\begin{aligned}
 \mathbb{P}(y_{n+1} \in \Gamma_k) &= \sum_{\pi_k \in \Pi_k} \mathbb{P}(y_{n+1} \in \Gamma_k, \pi_k) \\
 &= \sum_{\pi_k \in \Pi_k} \mathbb{P}(y_{n+1} \in \Gamma_k | \pi_k) \mathbb{P}(\pi_k) \\
 &= \sum_{i=k}^n \mathbb{P}(y_{n+1} \in \Gamma_k | \max_k(\pi_k) = i) \mathbb{P}(\max_k(\pi_k) = i) && (\mathbb{P}(\max_k(\pi_k) = i) = 0 \forall i < k) \\
 &= \sum_{i=k}^n \frac{i}{n+1} \mathbb{P}(\max_k(\pi_k) = i) \\
 &= \frac{1}{n+1} \sum_{i=k}^n i \mathbb{P}(\max_k(\pi_k) = i)
 \end{aligned}$$

where

$$\mathbb{P}(\max_k(\pi_k) = i) = \frac{\binom{i-1}{k-1}}{\binom{n}{k}}.$$

□

S.2 Additional Tables, Figures and Algorithms

Table S1: Combinations resulting in unique possible intersections in two dimensions.

1	2	3	4
+	+	+	+
-	+	+	+
+	-	+	+
+	+	-	+
+	+	+	-
-	-	+	+
-	+	-	+
-	+	+	-
-	-	-	-
+	-	-	-
-	+	-	-
-	-	+	-
-	-	-	+
+	+	-	-
+	-	+	-
+	-	-	+

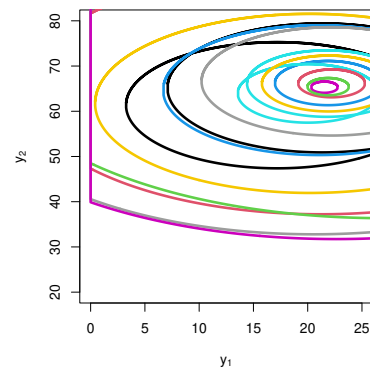
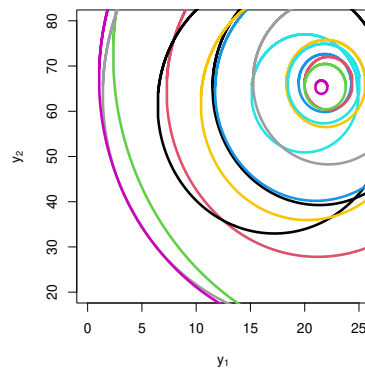
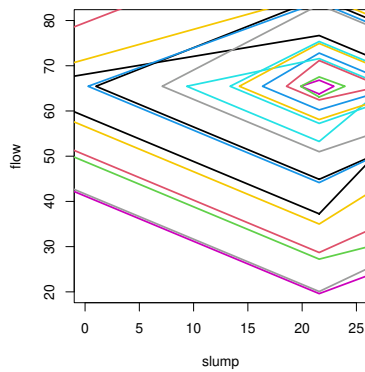


Figure S1: Intersections in two-dimensions for observations from single concrete test data point with 1-norm conformity measure (left) non-normalized 2-norm conformity measure (middle) and normalized ellipsoidal conformity scores (right).

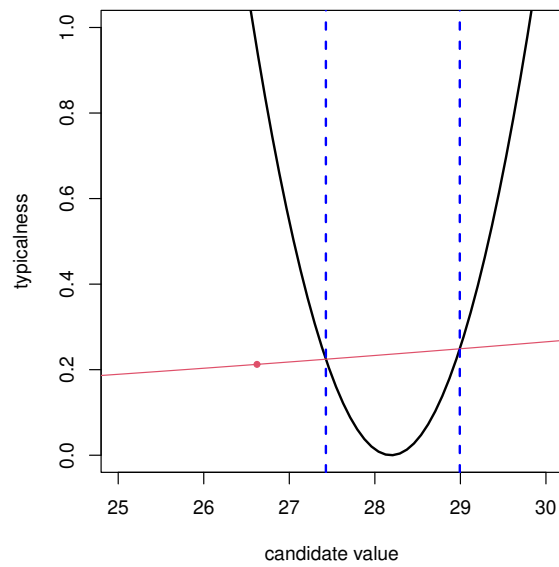


Figure S2: Constructing interval where conformity measure for  $(x_{n+1}, z)$  is less than score for observation  $i$ . Blue dotted lines show interval endpoints.

S.3 Additional Experiments

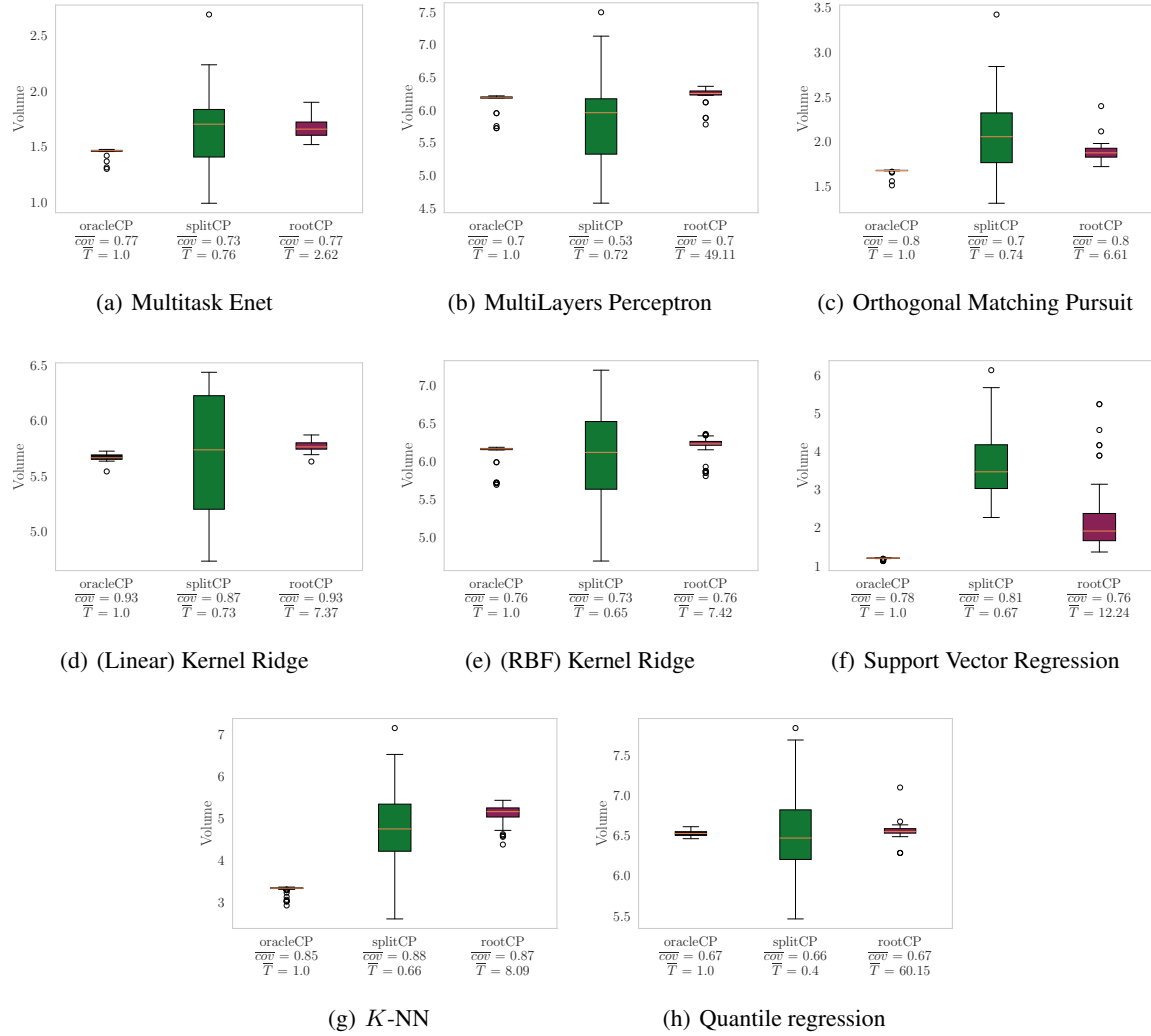


Figure S3: Benchmarking the convex Hull based conformal sets for several regression models on cement dataset. We display the lengths of the confidence sets over 100 random permutation of the data. We denoted  $\overline{cov}$  the average coverage, and  $\overline{T}$  the average computational time normalized with the average time for computing `oracleCP` which requires a single model fit on the whole data.

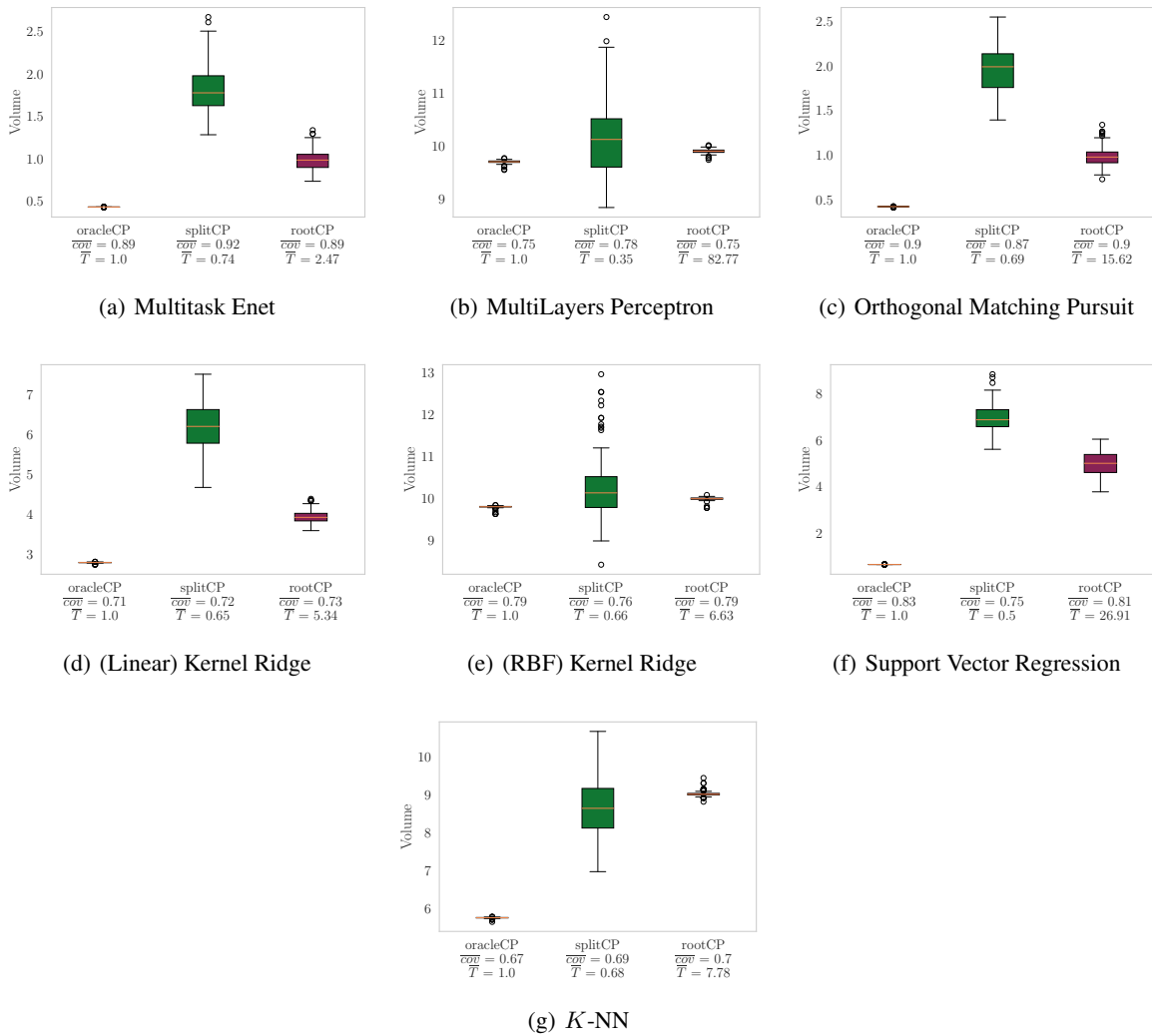


Figure S4: Benchmarking the ellipse based conformal sets for several regression models on synthetic dataset. We display the lengths of the confidence sets over 100 random permutation of the data. We denoted  $\overline{cov}$  the average coverage, and  $\overline{T}$  the average computational time normalized with the average time for computing oracleCP which requires a single model fit on the whole data.



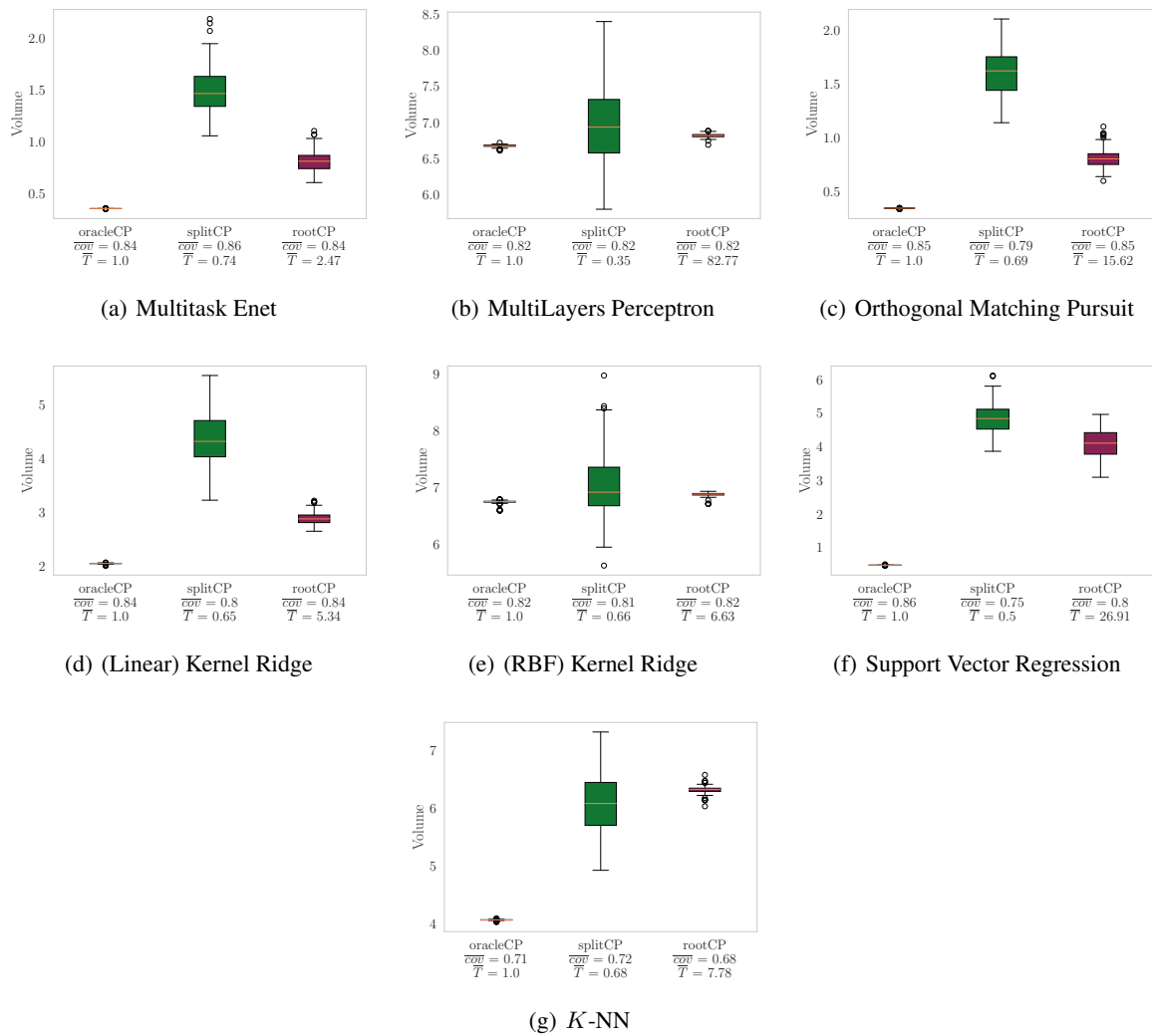


Figure S5: Benchmarking the convex Hull based conformal sets for several regression models on synthetic dataset. We display the lengths of the confidence sets over 100 random permutation of the data. We denoted  $\overline{cov}$  the average coverage, and  $\overline{T}$  the average computational time normalized with the average time for computing `oracleCP` which requires a single model fit on the whole data.

#### S.4 Pseudo-codes

We present more details on the proposed algorithms. The source codes will be available in open source later.

---

##### Algorithm 1 `exactCP-L1`

---

**Input:** data  $\mathcal{D}_n = \{(x_1, y_1), \dots, (x_n, y_n)\}$ , and  $x_{n+1}$

Coverage level  $\alpha \in (0, 1)$

Dimension  $d$

*# Initialization*

Construct  $H_k(x_{n+1})$  for each  $k = 1, \dots, d$ .

Construct  $a_{ki}, b_{ki}$  for all  $i = 1, \dots, n + 1$ .

Construct  $\mathcal{V}$ , defined as the set of  $2^{2d}$  ways to change the sign of each component  $|a_{ki} + b_{ki}z_k|$ .

*# Construct Conformity Measure Regions*

**for**  $i \in 1, \dots, n$  **do**

**for**  $v \in \mathcal{V}$  **do**

    We define the function  $v$  applied to  $S_i(z) - S_{n+1}(z)$  component-wise.

$$z_{0i}(v) = \{z : v(S_i(z) - S_{n+1}(z)) = 0\}$$

**end for**

1.  $\mathcal{Z}_i = \{z : z_{0i}(v) = z_{0i}(v') \text{ for some } v, v' \in \mathcal{V}\}$ .

*# Check Candidate Points*

**for**  $z \in \mathcal{Z}_i$  **do**

**if**  $S_{n+1}(z) \leq S_i(z)$  **then**

      add  $z$  to  $\mathcal{Z}_i^+$

**end if**

**end for**

$$\mathcal{E}_i = \tilde{\text{chull}}\{\mathcal{Z}_i^+\}$$

  where  $\tilde{\text{chull}}\{S\}$  is the convex hull built on set  $S$ .

**end for**

**Return:**  $\mathcal{E} = \{\mathcal{E}_i\}_{i=1}^n$

---

---

**Algorithm 2** rootCP in multiple dimensions

---

**Input:** data  $\mathcal{D}_n = \{(x_1, y_1), \dots, (x_n, y_n)\}$ , and  $x_{n+1}$

Coverage level  $\alpha \in (0, 1)$ , accuracy  $\epsilon_r > 0$ , list of search directions  $d_1, \dots, d_K$

*# Initialization*

Set  $z_0 = \mu_0(x_{n+1})$  where we fitted a model  $\mu_0$  on the initial training dataset  $\mathcal{D}_n$

*# Approximation of Boundary Points*

**for**  $k \in \{1, \dots, K\}$  **do**

We define the direction-wise conformity function as

$$\pi_k(t) = \pi(z(t)) - \alpha \text{ where } z(t) = z_0 + td_k$$

1.  $t^- = \text{bisection\_search}(\pi_k, t_{\min}, 0, \epsilon_r)$

2.  $t^+ = \text{bisection\_search}(\pi_k, 0, t_{\max}, \epsilon_r)$

Set  $\hat{\ell}_{d_k} = z_0 + t^- d_k$  and  $\hat{u}_{d_k} = z_0 + t^+ d_k$

**end for**

*# Convex approximation*

$$\hat{\Gamma}(x_{n+1}) = \tilde{\text{co}} \left\{ \hat{\ell}_{d_1}, \hat{u}_{d_1}, \dots, \hat{\ell}_{d_K}, \hat{u}_{d_K} \right\}$$

where  $\tilde{\text{co}}\{S\}$  is a convex set build on  $S$ , e.g., the convex hull or fit an ellipse using the points in  $S$

**Return:**  $\hat{\Gamma}(x_{n+1})$

---



---

**Algorithm 3** bisection\_search

---

**Input:** Function  $f$ , scalars  $a < b$  such that  $\text{sign}(f(a)) \neq \text{sign}(f(b))$ , accuracy  $\epsilon_r > 0$

Set  $\text{max\_iter} = \log_2\left(\frac{b-a}{\epsilon_r}\right)$

**for**  $i = 1$  **to**  $\text{max\_iter}$  **do**

$c = \frac{a+b}{2}$

**if**  $f(c) = 0$  or  $c - a \leq \epsilon_r$  **then**

**Return:**  $c$

**end if**

**if**  $f(c)f(a) < 0$  **then**

$b = c$

**else**

$a = c$

**end if**

**end for**

**Return:** the algorithm did not converge, increase  $\text{max\_iter}$ .

---